August, 2010

The Impacts of Miscanthus×Giganteus Production on the Midwest US Hydrologic Cycle

Andy VanLoocke, *University of Illinois at Urbana-Champaign*
Carl J. Bernacchi, *United States Department of Agriculture*
Tracy E. Twine, *University of Minnesota - Twin Cities*

GLOBAL CHANGE BIOLOGY
BIOENERGY

GCB Bioenergy (2010) **2**, 180–191, doi: 10.1111/j.1757-1707.2010.01053.x

The impacts of *Miscanthus* × *giganteus* production on the Midwest US hydrologic cycle

ANDY VANLOOCKE*, CARL J. BERNACCHI†‡ and TRACY E. TWINE§

*Department of Atmospheric Sciences, University of Illinois, 105 South Gregory St, Urbana, IL 61801, USA, †Department of Plant Biology, University of Illinois, 505 South Goodwin Ave, Urbana, IL 61801, USA, ‡USDA-ARS Global Change and Photosynthesis Research Unit, 1201 West Gregory Dr, Urbana, IL 61801, USA, §Department of Soil, Water, and Climate, University of Minnesota, 1991 Upper Buford Circle, 439 Borlaug Hall, St Paul, MN 55108, USA

Abstract

Perennial grasses are being considered as candidates for biofuel feedstocks to provide an alternative energy source to fossil fuels. *Miscanthus* × *giganteus* (miscanthus), in particular, is a grass that is predicted to provide more energy per sown area than corn ethanol and reduce net carbon dioxide emissions by increasing the storage of carbon belowground. Miscanthus uses more water than *Zea mays* (maize), mainly as a result of a longer growing season and higher productivity. Conversion of current land use for miscanthus production will likely disrupt regional hydrologic cycles, yet the magnitude, timing, and spatial distribution of effects are unknown. Here, we show the effects of five different scenarios of miscanthus production on the simulated Midwest US hydrologic cycle. Given the same historic precipitation observations, our ecosystem model simulation results show that on an annual basis miscanthus uses more water than the ecosystems it will likely replace. The actual timing and magnitude of increased water loss to the atmosphere depends on location; however, substantial increases only occur when miscanthus fraction cover exceeds 25% in dry regions and 50% in nearly all of the Midwest. Our results delineate where large-scale land use conversion to perennial biofuel grasses might deplete soil water resources. Given the fact that some watersheds within the Midwest already have depleted water resources, we expect our results to inform decisions on where to grow perennial grasses for biofuel use to ensure sustainability of energy and water resources, and to minimize the potential for deleterious effects to water quantity and quality.

Keywords: Agro-IBIS, biofuels, evapotranspiration, hydrology, land use change, miscanthus, modeling

Received 21 April 2010 and accepted 17 May 2010

Introduction

Miscanthus × *giganteus* (miscanthus) has been proposed as an ideal biomass feedstock for bioenergy production in the Midwest United States (Heaton *et al.*, 2008). Miscanthus is a naturally existing sterile hybrid native to Southeast Asia that was first grown in Europe in the 1930s (Lewandowski *et al.*, 2000) and has been considered a biomass energy candidate since the 1960s (Venendaal *et al.*, 1997). Miscanthus is a C_4 perennial rhizomatous grass (Lewandowski *et al.*, 2000) that is more productive than *Zea mays* (maize; Dohleman & Long, 2009) and requires fewer inputs (Beale & Long, 1997; Christian *et al.*, 2008; Miguez *et al.*, 2008). Because of the combination of high productivity and the ability to convert all of the aboveground cellulosic biomass to ethanol, miscanthus is predicted to reduce net carbon dioxide emissions (Stampfl *et al.*, 2007), produce more than double the renewable fuel per unit area than maize, and could help meet the Advanced Energy Initiative (AEI) goals by producing cellulosic ethanol from agriculture using ~9% of US cropland (Heaton *et al.*, 2008).

The effects of miscanthus production on the environment at the large scale are unknown. One of the primary concerns with miscanthus production is its potential to alter the hydrologic cycle through increases in evapotranspiration (ET; Stephens *et al.*, 2001; Hall, 2003; National Research Council Committee on Water

Correspondence: Tracy E. Twine, tel. +1 612 625 7278, fax +1 612 625 2208, e-mail: twine@umn.edu

Implications of Biofuels Production in the United States, 2008; Rowe *et al*., 2009; Smeets *et al*., 2009; Tilman *et al*., 2009). Miscanthus has been shown to have higher ET during the growing season relative to maize (Hickman *et al*., 2010, in press). It is likely that the observed differences are attributed to a number of factors including deeper and more extensive roots (Neukirchen *et al*., 1999), longer growing season (Beale & Long, 1995; Heaton *et al*., 2004), and higher leaf area index (LAI; Heaton *et al*., 2008). The potential impacts of increased water loss to the atmosphere as a result of land use change for biofuel production include but are not limited to decreases in streamflow (Donner *et al*., 2002), water table depth, and soil water storage (McIsaac *et al*., 2010, in press). To date, there is no direct assessment of the impacts of miscanthus production on the hydrologic cycle in the Midwest. Furthermore, no study has incorporated measurements of ET from miscanthus in the Midwest to evaluate model predictions. Given the expected differences in water use between miscanthus and current land cover, it is important to consider the potential changes in regional hydrology that are likely to occur if millions of hectares of land are converted to miscanthus production.

The goal of this study is to evaluate changes in Midwest US hydrology resulting from large-scale conversion from the existing land cover to one that contains miscanthus. We predict that altering the species composition from the existing land cover to include miscanthus will increase ET and alter the hydrologic cycle. Because of the scale in question and the lack of widespread measurements over the area of interest, we test this prediction through the use of the Integrated Biosphere Simulator – agricultural version (Agro-IBIS). Agro-IBIS is a dynamic global vegetation model (DGVM) that simulates the growth of natural vegetation and major US crops (i.e., maize, soybean, and spring and winter wheat). We modified Agro-IBIS to include a perennial biofuel feedstock system to represent miscanthus. This is the first such representation of a dedicated biofuel feedstock in a DGVM.

Methods

A new algorithm for miscanthus was created by integrating the existing Agro-IBIS C_4 grass algorithm with the crop management modules. The new algorithm was calibrated by adjusting relevant model parameters based on observations of miscanthus at the University of Illinois south farms (UISF; Table 1) and evaluated with observations at three locations in Illinois (Table 2). Regional simulations with the current land cover (Fig. 1) and miscanthus land cover scenarios were

Table 1 Agro-IBIS model parameters modified from default values for C_4 grass or maize to values representative for miscanthus

Parameter name	Description	Default value	New value	Sources
V_{max}	Maximum rubisco activity at 15 °C at top of canopy ($\mu mol\, m^{-2}\, s^{-1}$)	15	18	Dohleman & Long (2009)*
Q*	Intrinsic quantum efficiency (dimensionless)	0.5	0.46	Dohleman & Long (2009)
SLA	Specific leaf area ($m^2\, kg^{-1}$)	35	15	Dohleman & Long (2009)
LAI_{max}	Maximum LAI allowed	6.2	10.5	Heaton *et al*. (2008)
Lai_{cons}	LAI decline factor constant for crops	5	1.8	This paper
hyb_{gdd}	Maximum GDD (base 8 °C) required for physiological maturity	1600	3000	E. A. Heaton/F. G. Dohleman (unpublished results)
Mx_{mat}	Maximum number of days allowed past planting for physiological maturity to be reached	165	210	E. A. Heaton/F. G. Dohleman (unpublished results)
$Harv_{date}$	Harvest date	295	365	†
$ztop_{max}$	Canopy height maximum (m)	2.5	3.5	Heaton *et al*. (2008)
St_{suml}	Soil temperature summation GDD (base 0 °C) for emergence	1320	400	E. A. Heaton/F. G. Dohleman (unpublished results)
A_{leaf}	Fraction of assimilated carbon to leaves (initial, final)	0.4, 0.05	0.8, 0.1	This paper
A_{stem}	Fraction of assimilated carbon to stems (initial, final)	0.4, 0.1	0.1, 0.8	This paper
A_{root}	Fraction of assimilated carbon to roots (initial, final)	0.2, 0.2	0.1, 0.1	This paper
C_{cdays}	Consecutive days below killing temperature threshold	1	2	F. G. Dohleman (unpublished results)

*Value adjusted from 25 to 15 °C using the temperature correction in Bernacchi *et al*. (2001).

†An ideal harvest management strategy has not yet been identified. Thus a date representing the end of the calendar year was chosen arbitrarily.

GDD, growing degree days; LAI, leaf area index; SLA, specific leaf area.

Table 2 Summary of data available for model evaluation

Variable	Temporal resolution	Growing season(s)	Location(s)	Sources
A_n	Hourly	2005–2007	UISF	Dohleman & Long (2009), Dohleman *et al*. (2009)
LAI	Biweekly	2005, 2006	UISF	Heaton *et al*. (2008)
Yield	Annual	2004–2008	UISF, SB, SP	Heaton *et al*. (2008); F. G. Dohleman (unpublished results)
Latent heat flux	Daily	2007	UISF	Hickman *et al*. (2010, in press)

UISF, Urbana, IL: 40.04N, −88.22W "central region"; SB, Shabbona/Dekalb, IL: 41.84N, −88.85W "north region"; SP, Simpson/Robbs, IL: 37.45N, −88.72W "south region"; UISF, University of Illinois south farms; LAI, leaf area index.

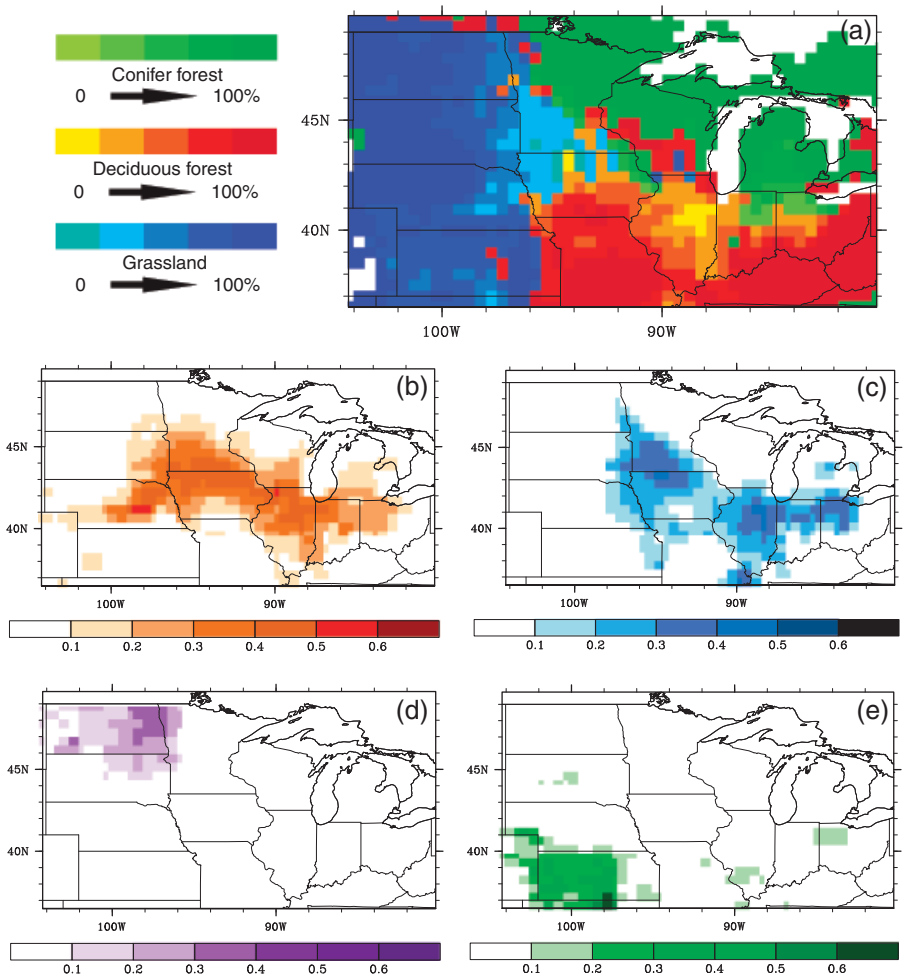

Fig. 1 Potential vegetation land cover classification and fraction cover as simulated by Agro-IBIS (a; valid 2002); fraction crop cover circa 1992, adapted from Donner (2003) for corn (b) soybean (c) spring wheat (d), and winter wheat (e).

conducted to examine the impact of large-scale miscanthus production on the hydrologic cycle.

Model description

Agro-IBIS is a DGVM adapted from IBIS (Foley *et al*., 1996; Kucharik *et al*., 2000) to simulate the growth and management of crops (Kucharik & Brye, 2003). Agro-IBIS and its predecessor have been evaluated extensively at multiple temporal and spatial scales representing most climate regimes. Evaluations include comparisons with satellite estimates of vegetation phenology (Twine & Kucharik, 2008) and regional and local measurements of soil moisture and temperature (Delire & Foley, 1999), surface energy fluxes (Delire & Foley, 1999; El Maayar *et al*., 2001; Kucharik & Twine, 2007),

crop yield (Kucharik, 2003), and river discharge and water balance (Kucharik *et al*., 2000; Lenters *et al*., 2000; Donner *et al*., 2002; Vano *et al*., 2006).

The number of soil layers is variable in Agro-IBIS, with each layer described by one of 11 soil texture classes (for this study eleven layers totaling 2.5 m in thickness were used). Agro-IBIS simulates water usage by depth (i.e., trees take up water from deeper soil layers than grasses; Foley *et al*., 1996). In addition, Agro-IBIS simulates a number of crop management practices (e.g. irrigation, fertilization, planting, harvesting). Simulations of leaf-level photosynthesis (Farquhar *et al*., 1980) and stomatal conductance (Collatz *et al*., 1991) are scaled to the canopy to simulate fluxes of carbon, water, and energy based on the land atmosphere physics presented in the land-surface transfer scheme (LSX) model (Thompson & Pollard, 1995a, b). Growth and development is dictated by phenological stages that are based on growing degree days (GDD).

The hydrologic cycle is simulated in Agro-IBIS as

$$T_{\mathrm{run}} = P - \mathrm{ET} - \mathrm{storage}, \tag{1}$$

where T_{run} is the sum of drainage through the soil column and surface runoff, P is precipitation, and storage is the sum of moisture stored in the soil column and on the canopy and ground surfaces. ET is the sum of transpiration from the vegetation canopy and evaporation from the soil surface and vegetation canopy. The same initial conditions (e.g. soil properties) and climate forcing for each independent grid cell as determined by the respective input datasets were used for each simulation in this study. Therefore, any changes in the hydrologic cycle are a result of differences in land cover in the respective simulations.

Implementation

Site-specific. We conducted the UISF simulations for a 4-year period using site-specific soil properties and meteorological driving data (i.e., air temperature, wind speed, radiation, precipitation, and relative humidity) from 2004 to 2007. A full description of the UISF site has been provided previously (Heaton *et al*., 2008; Dohleman & Long, 2009). Precipitation data were collected from Willard Airport (40.04N, −88.27W) while all other meteorological data were compiled from the nearest Surface Radiation Network (SURFRAD) site (40.05N, −88.37W) for 2002–2007. Missing SURFRAD data (0.55% of dataset) were filled with observations from the same hour with data collected at Willard Airport. Climatological datasets were used to spin-up the model until soil carbon pools reached near equilibrium.

Regional. The regional simulations were run at a $0.5^\circ \times 0.5^\circ$ spatial resolution over the Midwest United States (49.75N – 36.50N; −80.25W to −104.25W) and analyzed for the time period of 1941–2002. The land cover for each model grid cell is composed of fractions of crops and potential vegetation biomes (Fig. 1). Potential vegetation is the vegetation that would grow in the absence of human influence. In Agro-IBIS simulations, potential vegetation is initialized for each grid cell using the International Geosphere Biosphere Programme's 1-km DISCover land cover dataset (Loveland & Belward, 1997) and historical vegetation maps of natural ecosystems (Ramankutty & Foley, 1998). This map is updated at the end of each model year based on climate criteria (Foley *et al*., 1996). We define our current land cover with potential vegetation from the final model year run of 2002 combined with crop cover maps valid circa 1992 (Fig. 1).

The climate driver dataset was created by combining long-term (1901–2002) monthly mean climate data and 1961–1990 climatological mean values as given by the University of East Anglia Climate Research Unit datasets (CRU05; New *et al*., 1999; Mitchell & Jones, 2005) and anomalies of meteorological data for 1948–2002 from the National Centers for Environmental Prediction-National Center for Atmospheric Research (NCEP/NCAR) reanalysis dataset (Kalnay *et al*., 1996; Kistler *et al*., 2001). Hourly values were determined empirically using diurnal relationships of meteorological variables (Campbell & Norman, 1998).

Scenarios of miscanthus cover were created for fractions covers of 10%, 25%, 50%, 75%, and 100%. Miscanthus cover is expressed as a fraction of the land cover of every grid cell in the domain, regardless of the environmental or economic feasibility. It is uncertain where miscanthus will be grown and what vegetation it will replace. For this study, we assumed that miscanthus replaced existing vegetation in each grid cell based on its current composition. As an example for the 10% miscanthus cover scenario, if 90% of the grid cell is currently maize and 10% is deciduous forest, we replaced 9% of the maize and 1% of the forest with miscanthus. Grid cell values of simulated variables were calculated by weighting output according to the fraction of miscanthus and current cover present. For example, the grid cell value of ET for miscanthus production at 25% fraction cover was calculated as:

$$\mathrm{ET_{TOT}} = 0.25 \times \mathrm{ET_{MXG}} + 0.75 \times \mathrm{ET_{CUR}}, \tag{2}$$

where $\mathrm{ET_{TOT}}$ is the total grid cell value, $\mathrm{ET_{MXG}}$ is miscanthus ET, and $\mathrm{ET_{CUR}}$ is current vegetation ET. The current vegetation value is comprised of weighted

values of each land cover type that may include both natural vegetation and annual crops.

Parameterization. Key model parameters modified to represent miscanthus include specific leaf area (SLA), maximum rate of rubisco activity, intrinsic quantum efficiency, maximum canopy height, maximum leaf area index, and carbon allocation to leaf, stem, and root. Modeled carbon allocation fractions vary with development and were based on measurements of SLA, LAI, and aboveground biomass throughout the growing season. When possible, parameter values were chosen based on observations published previously (Table 1).

Evaluation. Key simulated variables evaluated include leaf photosynthesis (A_n), LAI, yield, and latent heat flux. Previously published data of biomass sampled several times per year (Heaton *et al.*, 2008; Dohleman & Long, 2009; F. G. Dohleman, unpublished results) were used to evaluate simulated annual values for 2004–2008. Hourly A_n was evaluated with observations taken several times throughout the growing season for 2005–2007 (Dohleman & Long, 2009; Dohleman *et al.*, 2009). Biweekly measurements of LAI (Heaton *et al.*, 2008) were used to evaluate simulated values throughout the 2005 and 2006 growing seasons. Simulated daily mean latent heat flux was evaluated with measurements collected over the 2007 growing season (Hickman *et al.*, 2010, in press).

Results

Model evaluation

Simulated hourly A_n corresponds with observed values and captures photosynthetic responses to meteorological forcing and phenotypic changes ($r^2 = 0.85$; slope = 0.99; Fig. 2). Simulated LAI throughout the growing season is similar to observations ($r^2 = 0.93$; slope = 1.02; Fig. 3a) and captures the increase early in the season, the maximal values, and the loss in LAI later in the season (Fig. 3b). The 4-year (2004–2007) mean simulated yield ($30.9 \pm 1.1\,\mathrm{Mg\,ha^{-1}}$) is similar to the observed value ($32.7 \pm 4.0\,\mathrm{Mg\,ha^{-1}}$; Fig. 4). Agro-IBIS simulates highest yield in 2006 ($33.6\,\mathrm{Mg\,ha^{-1}}$), which is also the year with the highest observed miscanthus yield in Central Illinois ($44.1 \pm 2.6\,\mathrm{Mg\,ha^{-1}}$). The CRU and NCEP/NCAR meteorological dataset ends in 2002 before observations of miscanthus are available for the Midwest US. Therefore, the most robust comparison of our long-term (1963–2002) mean regional values is with the mean of the only multiyear (2004–2008) biomass observation dataset. Across the state of Illinois, simu-

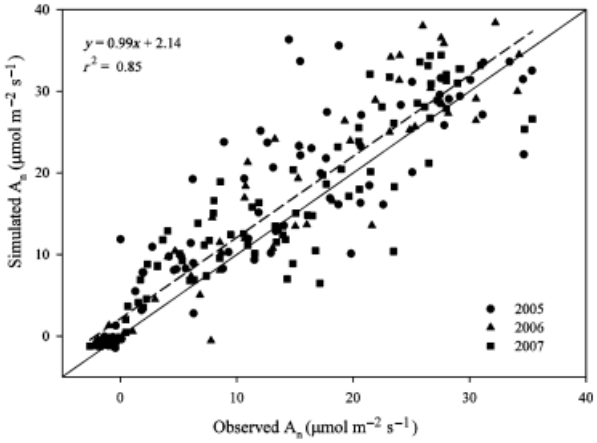

Fig. 2 Simulated and observed net leaf photosynthesis (A_n) for 249 hourly observations at various time periods over 31 days from 2005 to 2007. The dashed line is the linear regression line for all data; solid line is the 1 : 1 relationship.

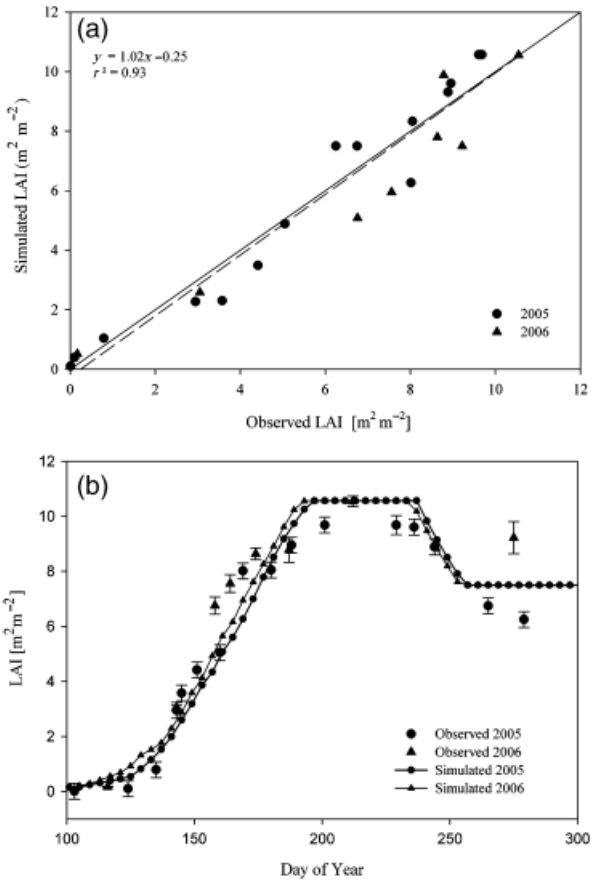

Fig. 3 Simulated and observed leaf area index (LAI) plotted against each other (a) and throughout the growing season (b). Observed values (from Heaton *et al.*, 2008) represent the mean of four observations and error bars represent 1 SE around the mean.

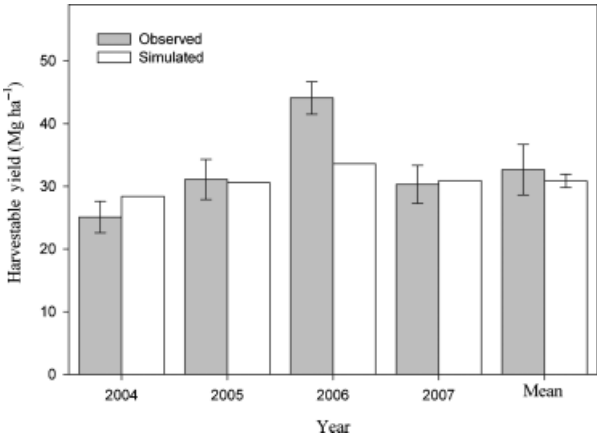

Fig. 4 Simulated and observed aboveground harvestable biomass for miscanthus grown at the University of Illinois south farms site. Observed values (from Heaton *et al.*, 2008 and Dohleman & Long, 2009) are mean ($n = 4$) $\pm$ 1 SE.

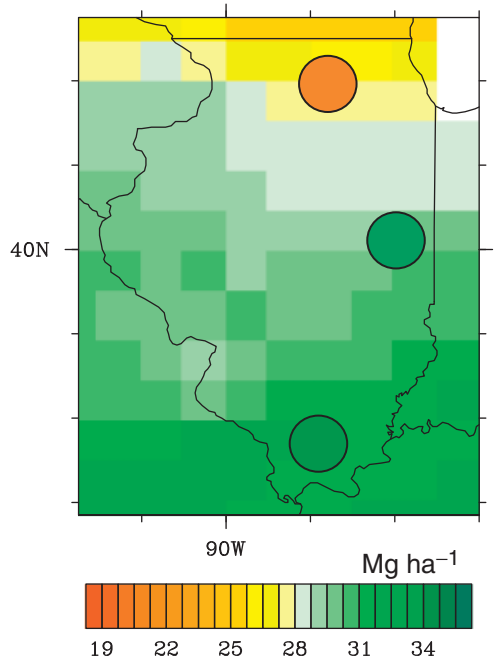

Fig. 5 Simulated 40-year (1963–2002) mean and the 3-year (2004–2006) mean observed (in circles; Heaton *et al.*, 2008) aboveground harvestable biomass for miscanthus in Illinois.

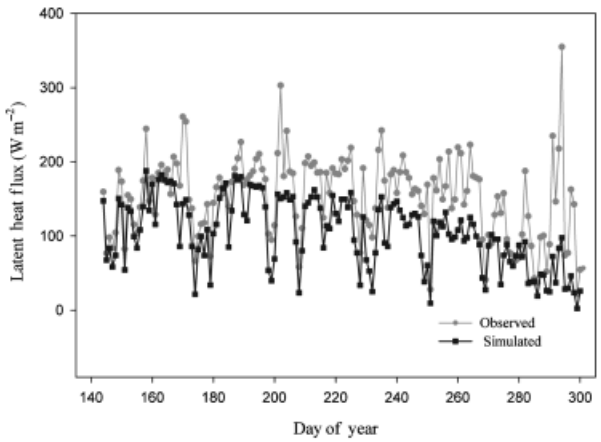

Fig. 6 Simulated and observed (from Hickman *et al.*, 2010, in press) daily mean latent heat flux for miscanthus over the 2007 growing season at University of Illinois south farms. Observations represent the mean of three replicates.

lated values range from 24 Mg ha^{-1} in the north to 33 Mg ha^{-1} in the south and correspond well with observed yield data (Fig. 5).

The observed mean daily latent heat flux over the growing season is 153.2 W m^{-2} day^{-1} and the simulated mean is 105.7 W m^{-2} day^{-1}. This difference is equivalent to 272 mm of water evapotranspired over the growing season. Variability in simulated daily mean latent heat flux is captured well throughout the growing season, with simulated values closely corresponding to daily maxima and minima (Fig. 6). While simulations capture the physiological responses to day-to-day changes in forcing, there is a consistent low bias in the simulated values.

Regional simulations

We present results as differences in 40-year mean simulated hydrologic components between the miscanthus cover scenarios and the current cover. The 40-year mean precipitation as well as the simulated 40-year mean ET and drainage for the current land cover are shown in Fig. 7. There is a general pattern of increased precipitation, ET, and to a lesser extent, drainage from the northwest corner to the southeast corner of the domain.

Differences in ET between the 100% miscanthus cover scenario and the current land cover scenario are evident over nearly the entire study domain (Fig. 8a). There exists variation in the areas of increased ET, with southern Missouri and western Kansas having little to no increase and a region extending from southwestern Minnesota to southern Kansas as well as Michigan showing increases that exceed 200 mm yr^{-1}. Other locations, including the highly productive Corn Belt (the area of high corn fraction cover in Fig. 1b), show increases that range between 50 and 150 mm yr^{-1}. Drainage is less in the 100% miscanthus simulation than for current cover over nearly the entire region, with decreases ranging from 50 to 250 mm yr^{-1} (Fig. 8b). The spatial pattern of differences in drainage is inverted relative to ET as a result of the current land cover simulation and all miscanthus scenario simulations

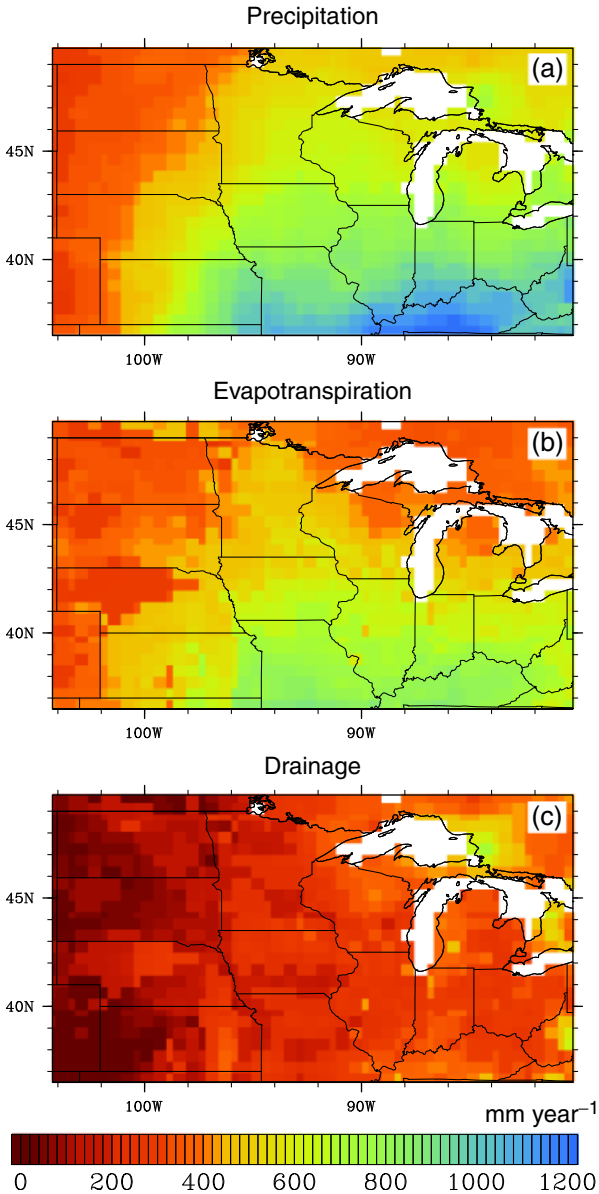

Fig. 7 Simulated 40-year (1963–2002) mean hydrologic cycle components of precipitation (a), evapotranspiration (b), and drainage (c) for current vegetation.

using the same precipitation dataset [see Eqn (1)]. Changes in surface runoff are negligible in the regional hydrological budget (Fig. 8c).

For most of the Midwest, the largest differences in ET and drainage between miscanthus and current vegetation occur during the time period when miscanthus is growing, with negligible differences outside of this period. In May, the differences in ET between the 100% miscanthus cover and the current land cover are variable across the domain (Fig. 9a). In drier regions (Fig. 7a) and where miscanthus is replacing annual crops (Fig. 1), increases range from 0.4 to greater than 2 mm day^{-1}. During the summer, the 100% miscanthus land cover shows consistent and widespread increases in ET relative to the existing land cover with largest increases in the northern evergreen needle leaf forests and grasslands of Nebraska and Kansas (Fig. 9b). Compared with May, the summer differences are diminished in the south and amplified in the north, which corresponds to emergence patterns. By September and October, a decline in transpiration of all vegetation types results in a homogeneous pattern of increases between 0.4 and 0.8 mm day^{-1} for miscanthus (Fig. 9c). As was observed with the annual means, the seasonal pattern of increases in ET is generally matched with corresponding decreases in drainage (Fig. 9d–f). However, there is slight variation in the spatial pattern of decreases in drainage relative to the increases in ET, with May and summer having fewer occurrences of statistically significant changes in the southeast region of the domain (Fig. 9d and e).

Given that more energy is going into ET, areas planted with miscanthus relative to current land cover will likely experience a cooling at the land surface. Furthermore, land cover change alters the reflectivity of the surface and the amount of radiation absorbed by the canopy, thereby impacting the surface energy budget. After accounting for differences in simulated reflectivity of the surface and the dynamical changes resulting from conversion to miscanthus, the model predicts decreases in annual mean sensible heat flux that range from 5 to 15 W m^{-2} over former cropland, to near 20 Wm^{-2} over former forest (Fig. 10a); and decreases in average annual canopy temperature that range from 0.5 °C over former cropland, to 0.8 °C over former forests (Fig. 10b). In grid cells where miscanthus replaces grassland, average canopy temperature increases in May by nearly 1 °C as the miscanthus begins its growing season before the existing grasses and absorbs more solar radiation. The long-term effects of such temperature adjustments are unknown but they have the potential to affect a number of temperature-sensitive ecosystem and biological processes.

When miscanthus is produced at 10% fraction cover, little to no changes occur in ET (Fig. 11a) and drainage (data not shown). At 25% miscanthus fraction cover, increases of 40–80 mm yr^{-1} in ET are found in portions of the Midwest (Fig. 11b). A marked change in ET occurs when fraction cover increases to 50% or greater. With 50% miscanthus coverage, the majority of the Midwest shows increases of 40–160 mm yr^{-1} (Fig. 11c). With 75% miscanthus cover, most of the Midwest shows increases >80 mm yr^{-1} with maximum increases of 200 mm yr^{-1} in the southwest region (Fig. 11d).

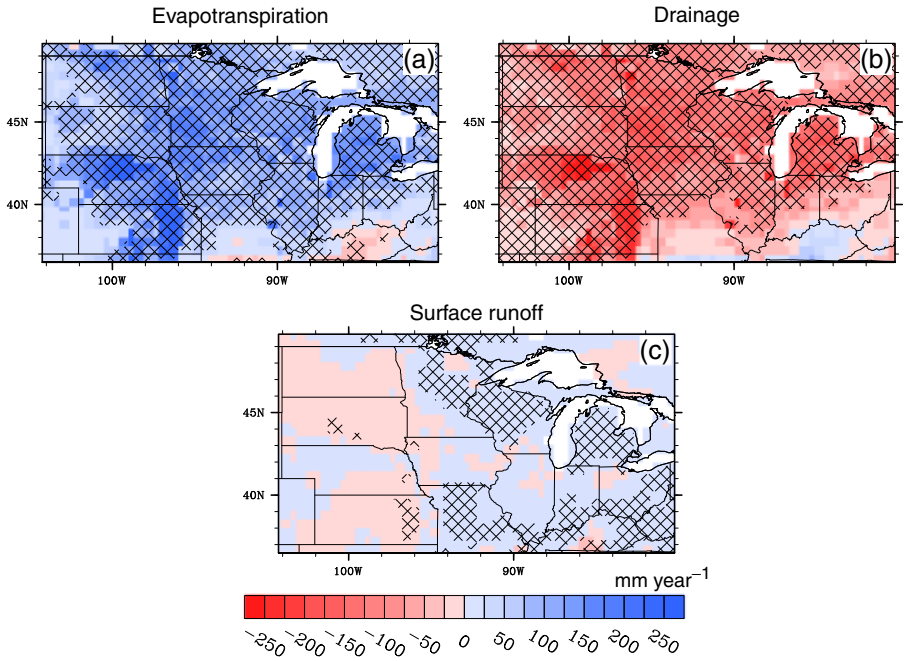

Fig. 8 Difference (100% miscanthus – current vegetation) in simulated 40-year (1963–2002) mean evapotranspiration (a), drainage (b), and surface runoff (c). Hatching indicates a statistically significant ($P<0.05$) difference according to Student's *t*-test.

Discussion

Simulations indicate minimal impacts on the hydrologic cycle at 10% miscanthus fraction cover. Considering that the AEI goals could be met by producing miscanthus on <10% of US agricultural land (Heaton *et al.*, 2008), uniform distribution of miscanthus over the Midwest US would have little to no impact on the hydrologic cycle. However, it has been proposed that the energetic and economic costs of producing energy from biomass would be minimized if biomass crops are planted in high fractions surrounding biorefineries in 'hot spots' and transported within the radius of US counties (Khanna *et al.*, 2008; Kim & Dale, 2008, 2009; Lambert *et al.*, 2008). Often in the Midwest, corn–soy rotations in agriculturally intense counties compose the majority of land cover. Therefore, if the model for production of corn ethanol is replaced with miscanthus, even given higher productivity, it is likely that fraction covers of miscanthus would exceed 25% or even 50%. If this scenario is realized, the results presented here indicate that significant changes in the hydrologic cycle would occur.

The results of these model scenarios show that the changes in hydrology are a function of differences in growing season length, leaf physiology, and maximum LAI. The higher ET for miscanthus relative to existing land cover is a consequence of miscanthus emergence in mid- to late April, a month or more earlier than most annual crops emerge (Fig. 9a). Higher ET from miscanthus continues into September and October (Fig. 9c) because of the lengthened growing season of miscanthus. In summer, the increased ET (Fig. 9b) is driven by a combination of higher LAI (Heaton *et al.*, 2008) and/or lower water use efficiency (Hickman *et al.*, 2010, in press).

Because Agro-IBIS simulates evaporation from the soil surface and vegetation canopy, simulated ET from miscanthus differs from that of other vegetation types as a result of differences in transpiration, differences in interception of water by the canopy, and differences in canopy shading of the soil surface. Analysis of these components of ET is beyond the scope of this study, however, our simulation results show greater transpiration from miscanthus than maize at the UISF site, which is in agreement with results of Hickman *et al.* (2010, in press). The model also predicts that evaporation of canopy-intercepted water from miscanthus is greater than that from maize but less than that of deciduous forest. Evaporation rates of canopy-intercepted water from miscanthus, though less than transpiration rates in our simulations, are significant and warrant further study as increases in this component of ET from land cover change imply an increased proportion of rainfall that is not available to the plant (Finch & Riche, 2010).

The results reported here are consistent with a number of previous studies representing a range of land use changes showing significant impacts on large-scale

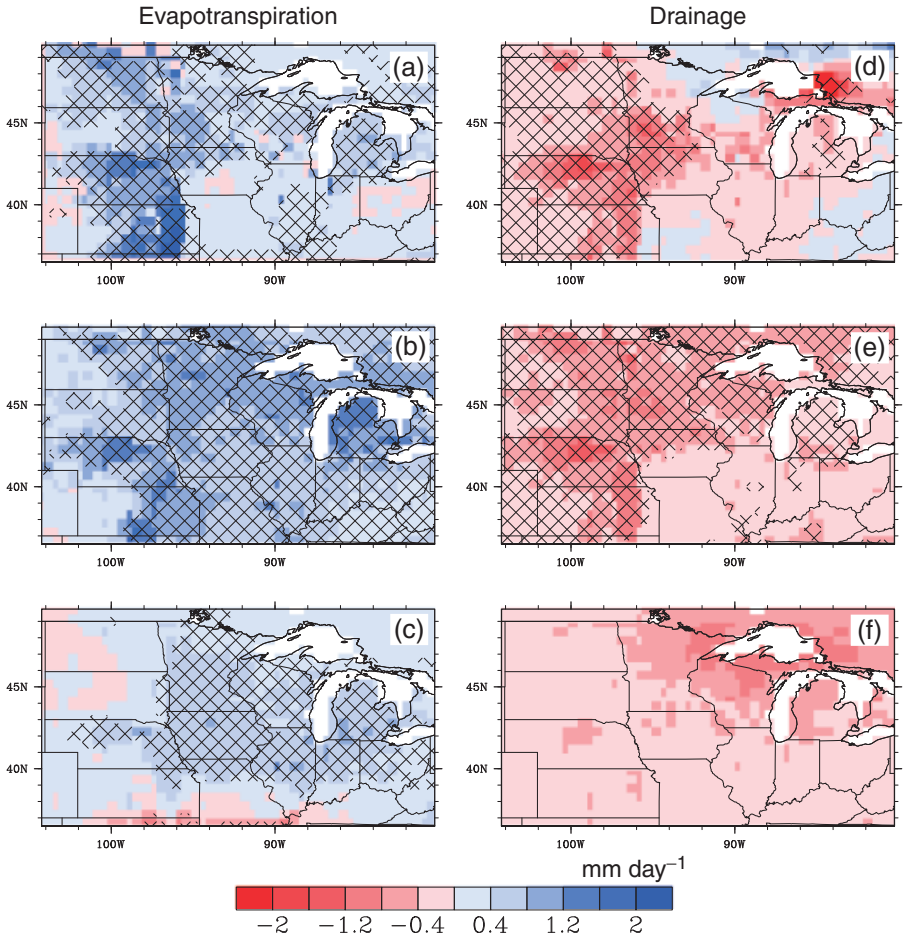

Fig. 9 Difference (100% miscanthus – current vegetation) in simulated 40-year (1963–2002) mean evapotranspiration (a, b, c) and drainage (d, e, f) for May (a, d), combined June, July, and August (b, e) and combined September and October (c, f). Hatching as in Fig. 8.

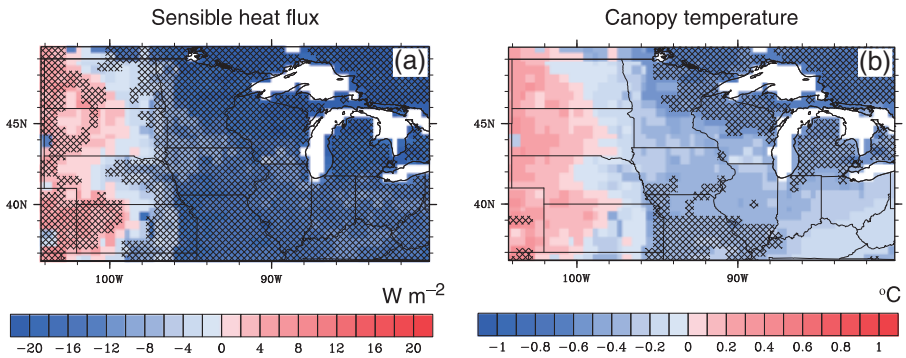

Fig. 10 Difference (100% miscanthus – current vegetation) in simulated 40-year (1963–2002) annual mean sensible heat flux (a) and canopy temperature (b). Hatching as in Fig. 8.

hydrology (Bosch & Hewlett, 1982; Bonan, 1997; Baron *et al.*, 1998; Snyder *et al.*, 2004; Twine *et al.*, 2004; Foley *et al.*, 2005). Twine *et al.* (2004) suggested that the large-scale conversion from native vegetation to the current annual crop-dominated cover may have reduced ET by ~75 mm yr^{-1} in the Corn-Belt. The increases in ET shown in our simulations suggest that miscanthus water use may be more similar to the past vegetation cover than the current cover. Changes in ET due to miscanthus production have also been predicted to

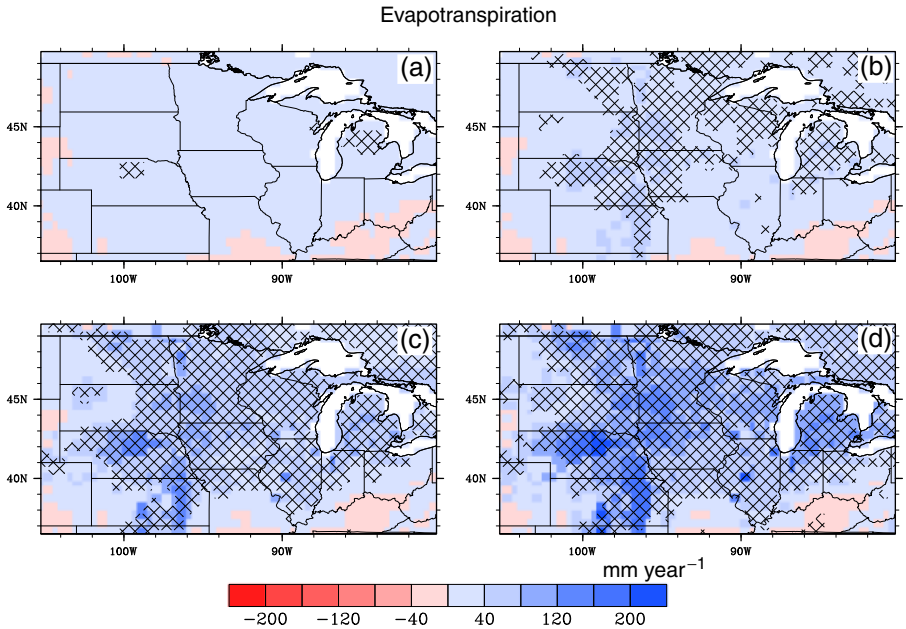

Fig. 11 Simulated difference (miscanthus – current vegetation) in 40-year (1963–2002) annual mean evapotranspiration for 10% (a), 25% (b), 50% (c), and 75% (d) fraction covers of miscanthus. Hatching as in Fig. 8.

affect local and regional climate by reducing sensible heat flux and near surface air temperature during the summer (Georgescu *et al.*, 2009). It is anticipated that a variety of biofuel feedstocks, chosen based on climate, soils, and hydrology, will be best suited to meet biomass needs, with miscanthus production focused in areas where water is less limiting (Heaton *et al.*, 2004).

While simulations agree well with most observations, latent heat flux is underestimated by the model (Fig. 6). The residual energy balance method for estimating latent heat flux used in this model evaluation forces closure in the energy budget and lumps error into latent heat flux. The most accurate measures of canopy fluxes seldom achieve $> \sim 80\%$ energy balance closure (Twine *et al.*, 2000; Wilson *et al.*, 2002; Oncley *et al.*, 2007); therefore, it is likely that ET estimated via the residual energy balance approach is biased high by at least 20%. Given this bias, it is possible that the simulations are closer to the actual fluxes than the evaluation presented here indicates. To test this, we regressed simulated latent heat flux with observations collected over a nearby cornfield and found Agro-IBIS to slightly overestimate LE (Agro-IBIS $= 1.08 \times$ obs-6.88; $r^2 = 0.80$) relative to eddy covariance observations, and to underestimate LE (Agro-IBIS $= 0.82 \times$ obs-16.95; $r^2 = 0.78$) relative to estimates from the residual method. While for the most part the simulations agree well with the variety of observations collected for miscanthus, the lack of mature field trials within the study domain could potentially limit the scalability of our results.

In this study we focus on changes in surface hydrology, yet alterations to the surface energy budget due to large-scale miscanthus production could potentially impact atmospheric processes and alter the intensity and distribution of precipitation (Jackson *et al.*, 2005). The potential feedbacks between miscanthus and the environment could drive large-scale changes in the hydrologic cycle over time and should be accounted for in future simulations.

Conclusion

The Agro-IBIS model was adapted to simulate the production of miscanthus, a proposed bioenergy feedstock for the Midwest US, to assess the impacts on hydrology. Simulations indicated statistically significant increases in ET and decreases in drainage over much of the Midwest for moderate cover fractions of miscanthus, however the extent varied based on percent miscanthus coverage and location. While we were able to quantify changes in hydrology for varying fraction covers, the long-term consequences to water resources and crop productivity for the Midwest remain uncertain. Future work should include coupled simulations of atmospheric and groundwater processes to improve the understanding of the impacts of biofuel production on hydrology and to assess the sustainability of biofuel production. The results of this analysis show that as the biofuel industry transitions to highly productive cellulosic feedstocks, it will be integral to account for the role

of water as a potential limiting factor in sustainable biofuel production.

Acknowledgements

We thank Santiago Vianna Cuadra for his help with algorithm development. We also thank Frank Dohleman, Emily Heaton, and George Hickman for supplying data for model validation. Don Ort, Jason Hill, Sarah Davis, Marcelo Zeri, and David Drag helped improve the manuscript. This study was funded by the Energy Biosciences Institute, University of Illinois at Urbana-Champaign.

References

Baron JS, Hartman MD, Kittel TGF, Band LE, Ojima DS, Lammers RB (1998) Effects of land cover, water redistribution, and temperature on ecosystem processes in the South Platte Basin. *Ecological Applications*, **8**, 1037–1051.

Beale CV, Long SP (1995) Can perennial C-4 grasses attain high efficiencies of radiant energy-conversion in cool climates. *Plant Cell and Environment*, **18**, 641–650.

Beale CV, Long SP (1997) Seasonal dynamics of nutrient accumulation and partitioning in the perennial C-4-grasses *Miscanthus × giganteus* and *Spartina cynosuroides*. *Biomass & Bioenergy*, **12**, 419–428.

Bernacchi CJ, Singsaas EL, Pimentel C, Portis AR, Long SP (2001) Improved temperature response functions for models of Rubisco-limited photosynthesis. *Plant Cell and Environment*, **24**, 253–259.

Bonan GB (1997) Effects of land use on the climate of the United States. *Climatic Change*, **37**, 449–486.

Bosch JM, Hewlett JD (1982) A review of catchment experiments to determine the effect of vegetation changes on water yield and evapo-transpiration. *Journal of Hydrology*, **55**, 3–23.

Campbell GS, Norman JM (1998) *An Introduction to Environmental Biophysics*, 2nd edn. Springer-Verlag, New York.

Christian DG, Riche AB, Yates NE (2008) Growth, yield and mineral content of *Miscanthus × giganteus* grown as a biofuel for 14 successive harvests. *Industrial Crops and Products*, **28**, 320–327.

Collatz GJ, Ball JT, Grivet C, Berry JA (1991) Physiological and environmental-regulation of stomatal conductance, photosynthesis and transpiration - a model that includes a laminar boundary-layer. *Agricultural and Forest Meteorology*, **54**, 107–136.

Delire C, Foley JA (1999) Evaluating the performance of a land surface/ecosystem model with biophysical measurements from contrasting environments. *Journal of Geophysical Research-Atmospheres*, **104**, 16895–16909.

Dohleman FG, Heaton EA, Leakey ADB, Long SP (2009) Does greater leaf level photosynthesis contribute to greater solar energy conversion efficiency in Miscanthus when compared to switchgrass? *Plant Cell Environment*, **32**, 1525–1537.

Dohleman FG, Long SP (2009) More productive than maize in the Midwest: how does miscanthus do it? *Plant Physiology*, **150**, 2104–2115.

Donner S (2003) The impact of cropland cover on river nutrient levels in the Mississippi River Basin. *Global Ecology and Biogeography*, **12**, 341–355.

Donner SD, Coe MT, Lenters JD, Twine TE, Foley JA (2002) Modeling the impact of hydrological changes on nitrate transport in the Mississippi River Basin from 1955 to 1994. *Global Biogeochemical Cycles*, **16**, 1043, doi: 10.1029/2001GB001396.

El Maayar M, Price DT, Delire C, Foley JA, Black TA, Bessemoulin P (2001) Validation of the integrated biosphere simulator over Canadian deciduous and coniferous boreal forest stands. *Journal of Geophysical Research-Atmospheres*, **106**, 14339–14355.

Farquhar GD, Caemmerer SV, Berry JA (1980) A biochemical-model of photosynthetic CO_2 assimilation in leaves of C-3 species. *Planta*, **149**, 78–90.

Finch JW, Riche AB (2010) Interception losses from Miscanthus at a site in south-east England – an application of the Gash model. *Hydrological Processes*, doi: 10.1002/hyp.7673.

Foley JA, DeFries R, Asner GP *et al*. (2005) Global consequences of land use. *Science*, **309**, 570–574.

Foley JA, Prentice IC, Ramankutty N *et al*. (1996) An integrated biosphere model of land surface processes, terrestrial carbon balance, and vegetation dynamics. *Global Biogeochemical Cycles*, **10**, 603–628.

Georgescu M, Lobell DB, Field CB (2009) Potential impact of US biofuels on regional climate. *Geophysical Research Letters*, **36**, L21806, doi: 10.1029/2009GL040477.

Hall RL (2003) *Grasses for Energy Production – Hydrological Guidelines*. Department of Trade and Industry (DTI), Centre for Ecology and Hydrology, London, UK.

Heaton EA, Dohleman FG, Long SP (2008) Meeting US biofuel goals with less land: the potential of miscanthus. *Global Change Biology*, **14**, 2000–2014.

Heaton EA, Voigt T, Long SP (2004) A quantitative review comparing the yields of two candidate C-4 perennial biomass crops in relation to nitrogen, temperature and water. *Biomass & Bioenergy*, **27**, 21–30.

Hickman GC, VanLoocke A, Dohleman FG, Bernacchi CJ (2010) A comparison of canopy evapotranspiration for maize and two perennial grasses identified as potential bioenergy crops. *Global Change Biology Bioenergy*, **2**, 157–168.

Jackson RB, Jobbagy EG, Avissiar R *et al*. (2005) Trading water for carbon with biological sequestration. *Science*, **310**, 1944–1947.

Kalnay E, Kanamitsu M, Kistler R *et al*. (1996) The NCEP/NCAR 40-year reanalysis project. *Bulletin of the American Meteorological Society*, **77**, 437–471.

Khanna M, Dhungana B, Clifton-Brown J (2008) Costs of producing miscanthus and switchgrass for bioenergy in Illinois. *Biomass & Bioenergy*, **32**, 482–493.

Kim S, Dale BE (2008) Life cycle assessment of fuel ethanol derived from corn grain via dry milling. *Bioresource technology*, **99**, 5250–5260.

Kim S, Dale BE (2009) Regional variations in greenhouse gas emissions of biobased products in the United States-corn-based ethanol and soybean oil. *International Journal of Life Cycle Assessment*, **14**, 540–546.

Kistler R, Kalnay E, Collins W *et al*. (2001) The NCEP-NCAR 50-year reanalysis: monthly means CD-ROM and documentation. *Bulletin of the American Meteorological Society*, **82**, 247–268.

Kucharik CJ (2003) Evaluation of a process-based Agro-Ecosystem Model (Agro-IBIS) across the US corn belt: simulations of the interannual variability in maize yield. *Earth Interactions*, **7**, 1–33.

Kucharik CJ, Brye KR (2003) Integrated BIosphere simulator (IBIS) yield and nitrate loss predictions for Wisconsin maize receiving varied amounts of nitrogen fertilizer. *Journal of Environmental Quality*, **32**, 247–268.

Kucharik CJ, Foley JA, Delire C *et al*. (2000) Testing the performance of a Dynamic Global Ecosystem Model: water balance, carbon balance, and vegetation structure. *Global Biogeochemical Cycles*, **14**, 795–825.

Kucharik CJ, Twine TE (2007) Residue, respiration, and residuals: evaluation of a dynamic agroecosystem model using eddy flux measurements and biometric data. *Agricultural and Forest Meteorology*, **146**, 134–158.

Lambert DM, Wilcox M, English A, Stewart L (2008) Ethanol plant location determinants and county comparative advantage. *Journal of Agricultural & Applied Economics*, **40**, 117–135.

Lenters JD, Coe MT, Foley JA (2000) Surface water balance of the continental United States, 1963–1995: regional evaluation of a terrestrial biosphere model and the NCEP/NCAR reanalysis. *Journal of Geophysical Research-Atmospheres*, **105**, 22393–22425.

Lewandowski I, Clifton-Brown JC, Scurlock JMO, Huisman W (2000) Miscanthus: European experience with a novel energy crop. *Biomass & Bioenergy*, **19**, 209–227.

Loveland TR, Belward AS (1997) The IGBP-DIS global 1 km land cover data set, DISCover: first results. *International Journal of Remote Sensing*, **18**, 3291–3295.

McIsaac GF, David MB, Mitchell CA (2010) *Miscanthus* and switchgrass production in central Illinois: impacts on hydrology and inorganic nitrogen leaching. *Journal of Environmental Quality*, in press.

Miguez FE, Villamil MB, Long SP, Bollero GA (2008) Meta-analysis of the effects of management factors on *Miscanthus* × *giganteus* growth and biomass production. *Agricultural and Forest Meteorology*, **148**, 1280–1292.

Mitchell TD, Jones PD (2005) An improved method of constructing a database of monthly climate observations and associated high-resolution grids. *International Journal of Climatology*, **25**, 693–712.

National Research Council Committee on Water Implications of Biofuels Production in the United States (2008) *Water Implications of Biofuels Production in the United States*. The National Academies Press, Washington, DC.

Neukirchen D, Himken M, Lammel J, Czyionka-Krause U, Olfs HW (1999) Spatial and temporal distribution of the root system and root nutrient content of an established Miscanthus crop. *European Journal of Agronomy*, **11**, 301–309.

New M, Hulme M, Jones P (1999) Representing twentieth-century space-time climate variability. Part I: development of a 1961–90 mean monthly terrestrial climatology. *Journal of Climate*, **12**, 829–856.

Oncley SP, Foken T, Vogt R *et al*. (2007) The energy balance experiment EBEX-2000. Part I: overview and energy balance. *Boundary-Layer Meteorology*, **123**, 1–28.

Ramankutty N, Foley JA (1998) Characterizing patterns of global land use: an analysis of global croplands data. *Global Biogeochemical Cycles*, **12**, 667–685.

Rowe RL, Street NR, Taylor G (2009) Identifying potential environmental impacts of large-scale deployment of dedicated bioenergy crops in the UK. *Renewable & Sustainable Energy Reviews*, **13**, 260–279.

Smeets EMW, Lewandowski IM, Faaij APC (2009) The economical and environmental performance of miscanthus and switchgrass production and supply chains in a European setting. *Renewable & Sustainable Energy Reviews*, **13**, 1230–1245.

Snyder PK, Delire C, Foley JA (2004) Evaluating the influence of different vegetation biomes on the global climate. *Climate Dynamics*, **23**, 279–302.

Stampfl PF, Clifton-Brown JC, Jones MB (2007) European-wide GIS-based modeling system for quantifying the feedstock from Miscanthus and the potential contribution to renewable energy targets. *Global Change Biology*, **13**, 2283–2295.

Stephens W, Hess T, Knox J (2001) *Review of the effects of energy crops on hydrology*. NF0416, Cranfield University, MAFF

Tilman D, Socolow R, Foley JA *et al*. (2009) Beneficial biofuels – the food, energy, and environment trilemma. *Science*, **325**, 270–271.

Thompson SL, Pollard D (1995a) A global climate model (Genesis) with a Land-Surface Transfer Scheme (Lsx) .1. Present climate simulation. *Journal of Climate*, **8**, 732–761.

Thompson SL, Pollard D (1995b) A global climate model (Genesis) with a Land-Surface Transfer Scheme (Lsx) 2. Co2 sensitivity. *Journal of Climate*, **8**, 1104–1121.

Twine TE, Kucharik CJ (2008) Evaluating a terrestrial ecosystem model with satellite information of greenness. *Journal of Geophysical Research-Biogeosciences*, **113**, G03027, doi: 10.1029/2007JG000599.

Twine TE, Kucharik CJ, Foley JA (2004) Effects of land cover change on the energy and water balance of the mississippi river basin. *Journal of Hydrometeorology*, **5**, 640–655.

Twine TE, Kustas WP, Norman JM *et al*. (2000) Correcting eddy-covariance flux underestimates over a grassland. *Agricultural and Forest Meteorology*, **103**, 279–300.

Vano JA, Foley JA, Kucharik CJ, Coe MT (2006) Evaluating the seasonal and interannual variations in water balance in northern Wisconsin using a land surface model. *Journal of Geophysical Research-Biogeosciences*, **111**, G02025, doi: 10.1029/2005JG000112.

Venendaal R, Jorgensen U, Foster CA (1997) European energy crops: a synthesis. *Biomass & Bioenergy*, **13**, 147–185.

Wilson K, Goldstein A, Falge E *et al*. (2002) Energy balance closure at FLUXNET sites. *Agricultural and Forest Meteorology*, **113**, 223–243.